

# We are IntechOpen, the world's leading publisher of Open Access books Built by scientists, for scientists

6,900

Open access books available

185,000

International authors and editors

200M

Downloads

Our authors are among the

154

Countries delivered to

TOP 1%

most cited scientists

12.2%

Contributors from top 500 universities



WEB OF SCIENCE™

Selection of our books indexed in the Book Citation Index  
in Web of Science™ Core Collection (BKCI)

Interested in publishing with us?  
Contact [book.department@intechopen.com](mailto:book.department@intechopen.com)

Numbers displayed above are based on latest data collected.  
For more information visit [www.intechopen.com](http://www.intechopen.com)



# A Monte Carlo Framework to Simulate Multicomponent Droplet Growth by Stochastic Coalescence

Lester Alfonso<sup>1</sup>, Graciela Raga<sup>2</sup> and Darrel Baumgardner<sup>2</sup>

<sup>1</sup>*Universidad Autónoma de la Ciudad de México, Mexico City,*

<sup>2</sup>*Universidad Nacional Autónoma de México  
México*

## 1. Introduction

The accurate modeling of the interactions between aerosols and cloud droplets for a multi-component system is a very difficult task in cloud modeling, since to express a variety of properties of the hydrometeors (such as the masses of water and soluble materials inside droplets) there is a need for multi-dimensional size distributions.

The aerosol distribution becomes important as the cloud drops evaporate and the solutes are recycled into aerosols that can serve as cloud condensation nuclei (CCN): the larger the mass of a hygroscopic aerosol, the lower the supersaturation needed to form a cloud droplet. In the marine environment, the aerosol recycling process is believed to be the major mechanism responsible for the bimodal shape of the aerosol size distributions (Flossmann, 1994; Feingold and Kreidenweiss, 1996). The heterogeneous chemical reactions, which add nonvolatile solute to each cloud droplet, strongly depend on the salt content and pH of the droplet (Alfonso and Raga, 2004). Since aerosols also have a significant influence on cloud microphysics and cloud radiative properties, it is necessary to simulate aerosol processes realistically and with adequate accuracy.

The usual approach adopted in detailed cloud microphysical modeling is to describe the aerosols and drops in two separate one-dimensional size distributions. Within this approach, only the average aerosol mass contained in drops of certain size is known, and it is not possible to accurately track the aerosol mass distribution within cloud droplets (Jacobson, 1999).

For the deterministic case (based on the solution of the kinetic collection or stochastic collection equation), the aerosol processing due to collision-coalescence was addressed by Bott (2000) by extending his previous model (Bott, 1998) to two-dimensional distributions. Within this framework each particle is characterized both by the mass of its dry aerosol nucleus and by its water mass. By adopting this framework, there is no need to parameterize the activation process.

Nevertheless, in real situations, there are several types of aerosols that act as CCN, and form an internal or an external mixture. Thus, the number of components of the system can be larger than two. The solution of the kinetic collection equation when the number of

components is larger than two is not an easy task and the alternative seems to be the stochastic treatment of the coalescence process (Alfonso et al., 2009).

Clouds that also contain ice crystals, as well as aerosols and cloud droplets, constitute even much more complex systems to be modeled. For mixed phase clouds, the components of the system are not only the particle mass and the aerosol mass inside the particles, but also the type of ice particle, such as ice crystals of different geometries (columns, plates, and dendrites), graupel or aggregates. In this case, the number of components in the system is very large and the kinetic framework is extremely difficult to implement. As a consequence, simplified treatments are adopted to deal with this problem. For example, in many models only one type of ice crystal is considered in order to make the problem more manageable.

Therefore, most models do not deal with several types of ice, and not take into account the aggregation of ice particles. When a variety of types of geometries are considered, then the system of kinetic equations can be actually very complex. For example, Khain and Sednev (1995) considered the interactions between water drops, columns, crystals (plate like crystals and dendrites), snowflakes, graupel and hail. The resulting system consists of seven complex kinetic equations that need to be solved with the Berry and Reinhardt (1974) method. In Alfonso et. al (2009), the algorithm of Gillespie (1976) for chemical reactions in the formulation proposed by Laurenzi et al. (2002) was applied to calculate the evolution of a two-component system (the masses of pure water and soluble material). The algorithm could be easily extended to any multi-component cloud system, with the possible inclusion of the ice phase.

Another less known drawback of the deterministic approach (based on the solution of the kinetic collection equation) is the fact that this equation can exhibit non-conservation of mass (gelation) under certain conditions. These limitations of the KCE are carefully analyzed in two previous papers (Alfonso et al, 2008 and Alfonso et al., 2010) by a direct comparison of numerical and analytical solutions of the KCE with true averages obtained with the stochastic method of Gillespie (1976). In these papers, a numerical criterion is proposed in order to calculate the validity time or breakdown time of the KCE.

Although it is easy to implement, the stochastic framework developed by Gillespie (1976) has an important limitation: It is computationally very expensive, and consequently, only small cloud volumes can be considered in the simulations. A possible solution to this problem can rely in the implementation of the grouping method (Ormel and Spaan, 2008) that allows modeling coalescence in a sufficiently large region.

This chapter is organized as follows. In section 2 we are concerned with drawbacks of the deterministic framework. Section 3 describes the multi-component collection stochastic algorithm and its application to solve kinetic collection equation. In Section 4 the multi-component stochastic algorithm is incorporated into a particle based microphysical model, and applied to model the microphysical evolution of an orographic cloud in Section 5. Section 6 summarizes the main results of the chapter.

## **2. Drawbacks of the deterministic approach**

### **2.1 Non conservation of mass after gelation**

One of the most important mechanisms for the formation of rain is the collision and coalescence of smaller droplets into larger ones. The deterministic approach to model this process is based in the solution of the kinetic collection (stochastic collection, coagulation) equation, which in discrete form is expressed as (Pruppacher and Klett, 1997):

$$\frac{\partial N(i,t)}{\partial t} = \frac{1}{2} \sum_{j=1}^{i-1} K(i-j,j)N(i-j)N(j) - N(i) \sum_{j=1}^{\infty} K(i,j)N(j) \tag{1}$$

where  $N(i,t)$  is the average number of droplets with mass  $x_i$  as a function of time. In Eq. (1), the time rate of change of the average number of droplets with mass  $x_i$  is determined as the difference between two terms: the first term describes the average rate of production of droplets of mass  $x_i$  due to coalescence between pairs of drops whose masses add up to mass  $x_i$ , and the second term describes the average rate of depletion of droplets with mass  $x_i$  due to their collisions and coalescence with other droplets.

The known limitations of the KCE are analyzed carefully in two papers (Alfonso et al., 2008 and Alfonso et al., 2010) by a direct comparison of numerical and analytical solutions of the KCE with true averages obtained with the stochastic method of Gillespie (1976). In these papers, a numerical criterion is proposed in order to calculate the validity time or breakdown time of the KCE.

The collision coalescence process is a stochastic one and is more accurately described by the stochastic coagulation equation for the joint probability distribution  $P(n_1, n_2, \dots, n_k, \dots, t)$  for the occupation numbers  $\bar{n}=(n_1, n_2, \dots, n_k, \dots)$  at time  $t$ . This equation has the form (Bayewitz et al., 1974; Lushnikov, 1978; Tanaka and Nakazawa, 1993; Inaba et al., 1999; Wang et al., 2006):

$$\begin{aligned} \frac{\partial P(\bar{n})}{\partial t} = & \sum_{i=1}^N \sum_{j=i+1}^N K(i,j)(n_i+1)(n_j+1)P(\dots, n_i+1, \dots, n_j+1, \dots, n_{i+j}-1, \dots; t) \\ & + \sum_{i=1}^N \frac{1}{2} K(i,i)(n_i+2)(n_i+1)P(\dots, n_i+2, \dots, n_{2i}-1, \dots; t) \\ & - \sum_{i=1}^N \sum_{j=i+1}^N K(i,j)n_i n_j P(\bar{n}; t) - \sum_{i=1}^N \frac{1}{2} K(i,i)n_i(n_i-1)P(\bar{n}; t) \end{aligned} \tag{2}$$

In (2)  $n_i$  is the number of droplets with mass  $x_i$ , and  $N$  is the total number of size bins. The KCE results from taking the first moments::

$$\langle n_k \rangle = \sum_{\bar{n}} n_k P(\bar{n}; t) \tag{3}$$

and assuming that  $\langle n_i n_j \rangle = \langle n_i \rangle \langle n_j \rangle$ . Under these assumptions Eq.(2) reduces to the kinetic collection equation (1). Then, the average spectrum obtained from Eq.(1), and the ensemble average obtained from different realizations of the stochastic collection process are different. Bayewitz et al. (1974) showed that the solution of the KCE and the expected values calculated from the stochastic equation are equal only if the covariances are omitted from the probabilistic model.

Equation (1) is not expected to be accurate when the initial number of particles is small, or if  $K(i,j)$  increases sufficiently rapidly with  $x_i$  and  $x_j$ . For example, in the analytic solution for the case  $K(i,j)=C x_i \times x_j$ , with monodisperse initial conditions  $N(1,0)=N_0$ , the total mass starts to decrease after a certain time and there is an increase in the second moment. Drake (1972) calculated the analytical solutions of the KCE for polynomials of the form  $K(x,y)=Cxy$ . In this case the second moment evolution is given by:

$$M_2(\tau) = \frac{M_2(t_0)}{1 - CM_2(t_0)\tau} \quad (4)$$

Where  $M_2(\tau)$  defined by the expression (for the discrete case):

$$M_2(t) = \sum_{i=1}^{N_d} x_i^2 N(i,t) \quad (5)$$

Where  $N_d$  is the total number of size bins. Note that when

$$\tau = [CM_2(t_0)]^{-1} \quad (6)$$

The second moment  $M_2$  is undefined and the total mass of the system starts to decrease. This is usually interpreted to mean that a macroscopic runaway particle has formed (known as a gel). The product kernel  $K(i,j) = Cx_i \times x_j$  is the prototype example where the process exhibits a phase transition (also called gelation). After gelation occurs, there is a transition from a continuous system to one with a continuous distribution *plus* a massive runaway particle. The critical time is defined in terms of the existence of solutions of the coagulation equation (1) which is mass-conserving.  $T_{gel}$  is the largest time such that the discrete model has a solution with  $M_1(t) = M_1(0)$  for  $t < T_{gel}$  and  $M_1(t) < M_1(0)$  for  $t > T_{gel}$ .

As analytical expressions for the gelation time only exist for very simple kernels, it can be estimated (for real kernels relevant to cloud physics) using a Monte Carlo method (Alfonso et al., 2008, 2010), based on the original algorithm proposed by Gillespie (1976). Following the conjecture made by Inaba et al. (1999), the  $T_{gel}$  is estimated as the maximum of the ratio of the standard deviation for the largest particle mass over all the realizations, to the averaged value evaluated from the realizations of the stochastic algorithm:  $M_{L1,S} = \text{STD}(M_{L1}) / M_{L1}$ . The standard deviation for the largest droplet mass is calculated for each time by using the expression:

$$\text{STD}(M_{L1}) = \sqrt{\frac{1}{N_r} \left( \sum_{i=1}^{N_r} (M_{L1}^i - M_{L1})^2 \right)} \quad (7)$$

where  $M_{L1}$  is the ensemble mean of the mass of the largest droplet over all the realizations (given by Eq. (17)),  $N_r$  is the number of realizations of the Monte Carlo algorithm and  $M_{L1}^i$  is the largest droplet for each realization.

In Alfonso et al. (2008) the gel transition time  $\tau$  for an initial monodisperse distribution of 100 droplets of 14  $\mu\text{m}$  in radius (droplet mass  $1.1494 \times 10^{-8}\text{g}$ ) was estimated from analytical solutions and from Monte Carlo simulations. The volume of the cloud was set equal to 1  $\text{cm}^3$ . Using a value of  $C = 5.49 \times 10^{10} \text{cm}^3 \text{g}^{-2} \text{s}^{-1}$ , then  $\tau$  in (6) is 1379 sec. For the same analytical conditions, the behavior of  $M_{L1,S}$  was calculated from 1000 realizations ( $N_r = 1000$ ) of the Monte Carlo algorithm. The results are displayed in Fig. 1. The maximum of  $\sigma_L$  was obtained for  $\tau = 1335$  sec, very similar to the analytical estimation from Eq. (6), indicating that the statistic parameter in Eq. (7) is a good estimate of the transition to gel.

For more realistic kernels, relevant to cloud physics modeling, the validity time can be estimated in a similar manner. Alfonso et al. (2010) estimated the breakdown of the coagulation equation for the hydrodynamic kernel:

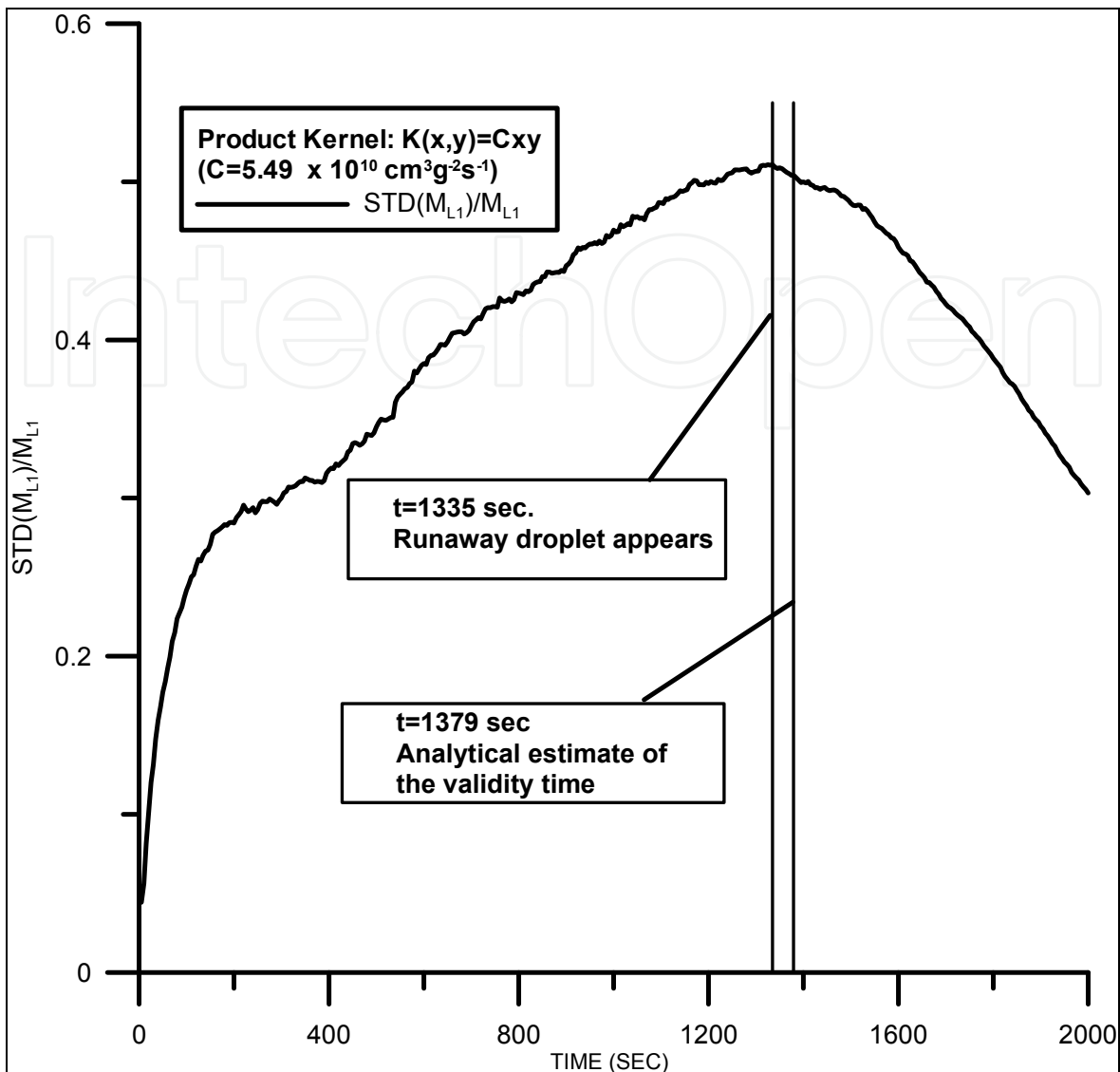


Fig. 1. The ratio (defined in Eq. 7) as a function of time, for the product kernel  $K(x,y)=Cxy$ , ( $C=5.49 \times 10^{10} \text{ cm}^3 \text{ g}^{-2} \text{ s}^{-1}$ ). Note that  $STD(M_{L1})/M_{L1}$  reaches a maximum when the runaway droplet appears.

$$K(x,y) = \pi [R(x) + r(y)]^2 E(x,y) [V(x) - V(y)], \quad x \geq y \quad (8)$$

where  $V(x), V(y)$  and  $R(x), r(y)$  are the terminal velocities and radiuses of droplets with masses  $x$  and  $y$  respectively, and the values of the collision efficiencies  $E(x,y)$  were taken from Hall (1980). The behavior of the ratio  $M_{L1,S}$  (Eq. 7) was evaluated from 1000 realizations of the Monte Carlo algorithm, and the time when the maximum of the statistics (7) was reached compared with the time when the liquid water content (LWC), obtained numerically with a finite difference scheme, starts to decrease.

A cloud volume of  $1 \text{ cm}^3$  was simulated, that initially contained a bidisperse droplet distribution: 50 droplets of  $14 \mu\text{m}$  in radius, and 50 droplets of  $17.6 \mu\text{m}$  in radius. Figure 2 shows that the liquid water content (or total mass) of the system is no longer conserved after 800 sec. This time is very close to the time when the statistics  $M_{L1,S}$  determined from the Monte Carlo realizations, reaches its maximum (850 sec).

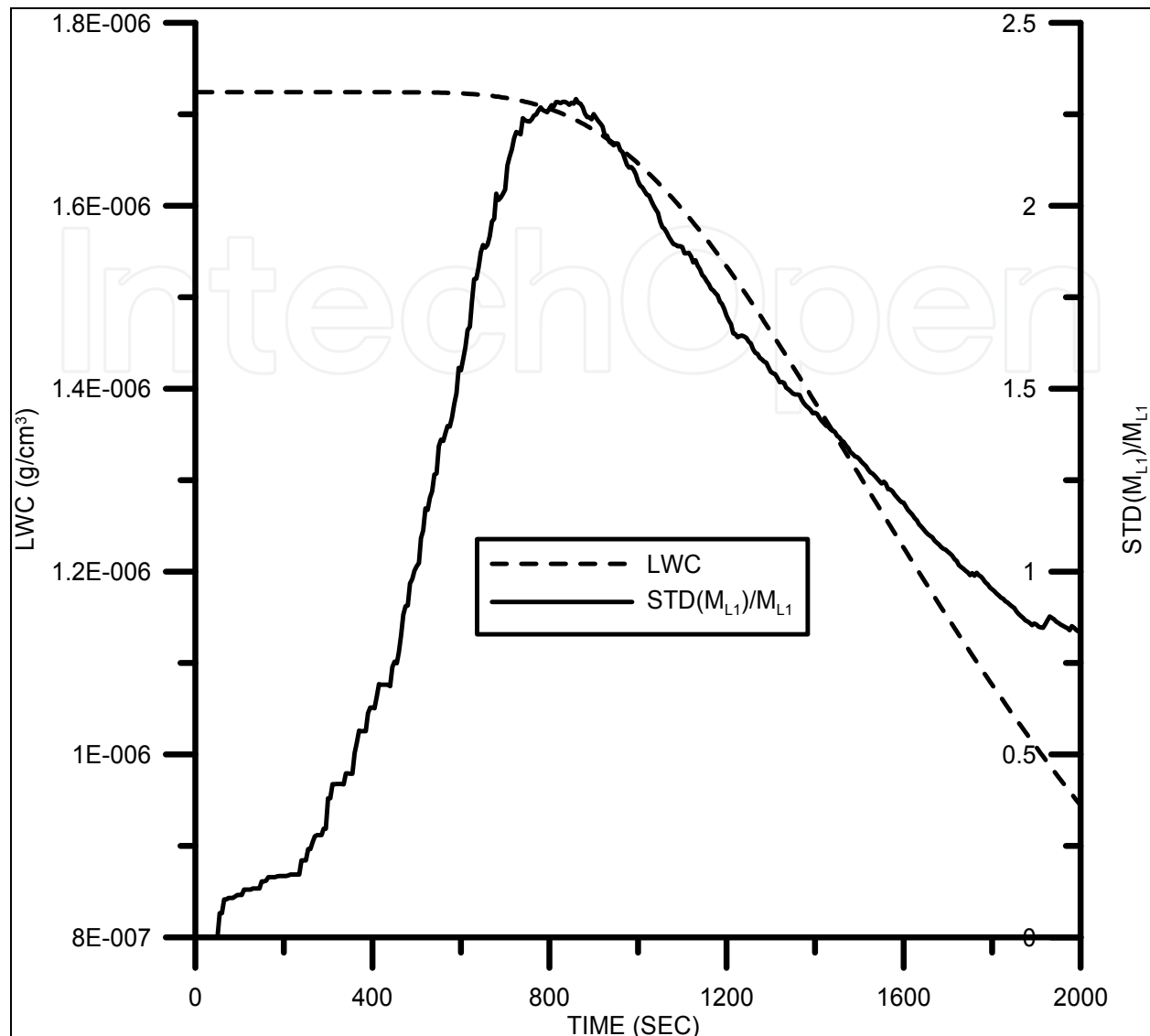


Fig. 2. Time evolution of total liquid water content calculated from the numerical solution of the KCE for the hydrodynamic kernel (dashed line) and the statistics  $STD(M_{L1})/M_{L1}$  (solid line) estimated from the Monte Carlo algorithm. The simulations were performed for the hydrodynamic kernel with a bidisperse initial condition  $N(1;0)=50$  and  $N(2;0)=50$ .

A second simulation was performed, with twice the initial number of droplets, and again the results show a good correspondence between the time of the  $M_{L1,S}$  maximum (430 sec.) and the gelation time obtained from the numerical solution of the KCE (415 sec.). These results confirm the fact that total mass calculated assuming a continuous droplet distribution starts to decrease around the time when the runaway droplet appears.

### 3. Stochastic approach for the collection process

#### 3.1 Definition of species and multi-component stochastic collection algorithm

Within the stochastic framework, each species represents a large number of hydrometeors with the same attributes and position. These attributes are: a) the type of particle

(unactivated and activated droplets, and ice crystals of different geometries), b) the particle mass, and c) the dry aerosol mass for each substance.

Warm clouds are composed of only one type of hydrometeor since unactivated CCN in equilibrium at a given supersaturation and activated droplets are treated as particles of the same type. In this case the attributes are only the droplet mass and the mass of dry aerosols. In a multi-component system, each species is characterized by a vector of properties  $\bar{u}_\mu = (u_1, u_2, \dots, u_N)$ , such that, a droplet with composition  $\bar{u}_\mu$  is a member of the  $\mu$ th species. After time  $t=0$  the species will randomly coalesce according to:

$$A_{u_1, u_2, \dots, u_N} + B_{u'_1, u'_2, \dots, u'_N} = C_{u_1 + u'_1, u_2 + u'_2, \dots, u_N + u'_N} \tag{9}$$

where  $A_{u_1, u_2, \dots, u_N}$  and  $B_{m'_a, m'_{a_1}, m'_{a_2}, m'_{a_3}}$  are droplets with compositions  $\bar{u}_\mu = (u_1, u_2, \dots, u_N)$  and  $\bar{u}'_\mu = (u'_1, u'_2, \dots, u'_N)$ , respectively. The transition probabilities for coalescence events follow Laurenzi et al. (2002) and are given by:

$$a(i,j) = V^{-1}K(i,j)N_iN_jdt \equiv \text{Pr}\{ \text{Probability that two particles of species } i \text{ and } j \text{ (for } i \neq j) \text{ with populations (number of particles) } N_i \text{ and } N_j \text{ will collide within the imminent time interval} \} \tag{10}$$

$$a(i,i) = V^{-1}K(i,i)\frac{N_i(N_i-1)}{2}dt \equiv \text{Pr}\{ \text{Probability that two particles of the same species } i \text{ with population (number of particles) } N_i \text{ collide within the imminent time interval} \} \tag{11}$$

In (10) and (11),  $K(i,j)$  is the collection kernel,  $V$  is the cloud volume; and  $N_i$  and  $N_j$  are the total number of droplets for the species  $i$  and  $j$ . An index is assigned to each species (particles with a specific  $\bar{u}_\mu = (u_1, u_2, \dots, u_N)$  composition). Within this framework, there is a unique index  $\nu$  for each pair of droplets  $i, j$  that may collide. For a system with  $N_s$  species  $(S_1, S_2, \dots, S_N)$   $\nu \in \frac{N_s(N_s+1)}{2}$ . The set  $\{\nu\}$  defines the total collision space, and is equal to the total number of possible interactions. The transition probabilities (10) and (11) are then represented by one index ( $a_\nu$ ).

In Alfonso et al. (2009) the stochastic algorithm of Laurenzi et al. (2002) was implemented to calculate two-component droplet growth. This version of the algorithm is difficult to implement in cloud microphysical models, that considered a constant time step. Consequently, a modification is introduced following Sue et al. (2007). First the number of collisions occurring during a time step  $\Delta t$  is determined from the expression:

$$C_T = \frac{\Delta t \sum_{i=1}^{N_s} \sum_{j=1}^{N_s} K(i,j)N_iN_j}{V} \tag{12}$$

Where  $N_s$  is the total number of species. Then, the collision pairs are selected by generating  $C_T$  random numbers  $r_i$  from a uniform distribution in the interval  $(0, 1)$ , and the indexes  $\nu$  for the  $C_T$  collisions determined from the inequality:



$$\sum_{v=1}^{\mu-1} a_v < r_i \alpha < \sum_{v=1}^{\mu} a_v \quad (13)$$

Where  $\alpha = \frac{N_s(N_s+1)}{\sum_{v=1}^2 a_v}$  (14) and  $i=1, \dots, C_T$ . After each collision event, the size distribution is updated by taking into account:

$$N_i = N_i - 1, \quad N_j = N_j - 1 \quad (14)$$

If new species are created, then ( $N_s = N_s + 1$ ). For the new species, the droplet and aerosol masses for each component are equal to the sum of the droplet and aerosol masses of the colliding droplets following Eq. (9). The Monte Carlo algorithm can be summarized as follows:

1. At  $t=0$ , the event counter is set to zero and the initial number of species  $N_1, N_2, \dots, N_N$  is defined.
2. The total number ( $C_T$ ) of collisions in the time interval  $\Delta t$  are determined from the expression (12).
3. Generate  $C_T$  random numbers from a uniform distribution and determine the  $N_T$  collision indexes from (13).
4. Change the numbers of species to reflect the execution of  $C_T$  collisions.
5. Return to step 2.

The approach follow by Sun et al. (2007) was adopted and only a single stochastic experiment was run. This can be justified by considering that the statistical error is proportional to  $1/\sqrt{N_{\text{droplets}}}$ , where  $N_{\text{droplets}}$  is the total number of droplets in the coalescence volume. Then, in order to reduce the statistical error, volumes larger than  $10^3 \text{ cm}^3$  are considered in our simulations. This problem was carefully studied by Laurenzi et al. (2002). They found that the differences between the KCE and the results of the Monte Carlo for one single realization were almost negligible for sufficiently large coalescence volumes.

In order to check the performance of the previously described Monte Carlo algorithm, a simulation with the sum kernel ( $K(i,j)=B(x_i+x_j)$ ) was performed and compared with the analytical solution of the one-component kinetic collection equation derived by Scott (1968) for a monodisperse initial condition.

$$N(t) = N_0(1 - T) \quad (15a)$$

$$T = 1 - \exp(-BN_0v_0t) \quad (15b)$$

In Eqs. 15a,b  $N_0$  and  $v_0$  correspond to the initial number and volume of droplets, respectively. We simulate a cloud volume equal to  $5000 \text{ cm}^3$ , containing  $5 \times 10^5$  droplets ( $N_0$ ) of  $14 \mu\text{m}$  in radius ( $v_0=1.1494 \times 10^{-8} \text{ cm}^3$ ). Following Long (1974), a value of  $8.83 \times 10^2 \text{ cm}^3 \text{ g}^{-1} \text{ s}^{-1}$  was assumed for constant  $B$  in the sum kernel. The results obtained for the total concentration can be checked in Fig. 3, with a good correspondence between the analytical and the Monte Carlo results.

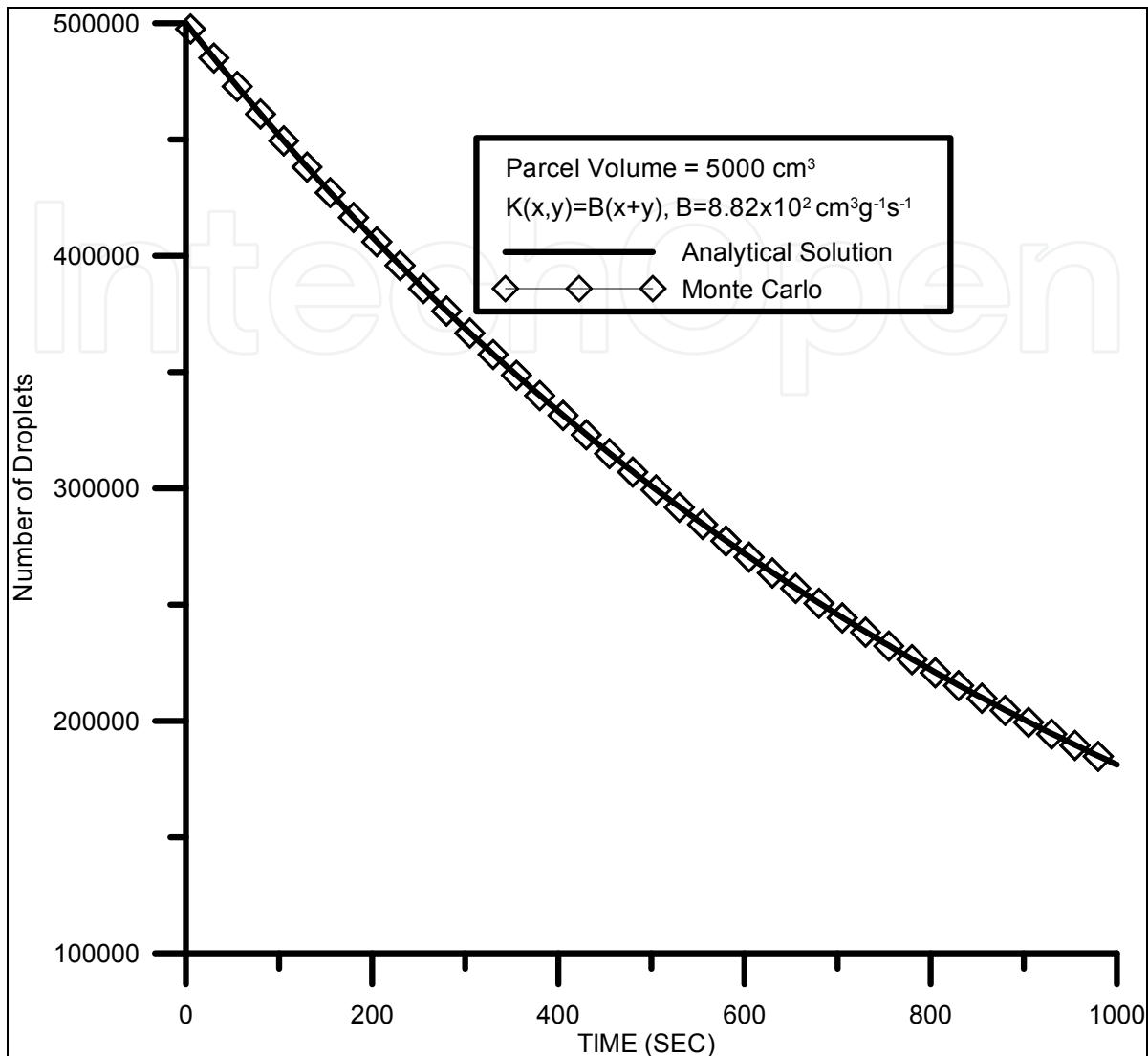


Fig. 3. Time evolution of the total number of particles obtained from the MC method (diamonds), versus the analytical solution of the kinetic collection equation (solid line).

### 3.2 The grouping method

Since the total collision rate  $C_T$  (see equation 12) is proportional to the number of particles, we can conclude that the application of the stochastic approach in systems involving a large number of particles and with only two physical particles colliding per MC cycle is highly impractical.

The procedure previously described is not very useful when simulating a cloud large volume, because of the high cost in computation. For example, in a three dimensional cloud model the typical coalescence cell has a volume of  $10^9 \text{ cm}^3$  and considering a droplet concentration at cloud base typical of maritime clouds ( $10^2 \text{ cm}^{-3}$ ), then the number of droplets will be about  $10^{11} \text{ cm}^{-3}$ . A possible solution to this problem relies in the implementation of the grouping method developed by Ormel and Spaans (2008), where particles of the same species are divided into groups and only collisions between groups of identical particles are considered in a MC cycle.

A similar approach for the stochastic collection (the Super Droplet method) was proposed by Shima et al. (2007). They defined collision between Super Droplets (that are actually species): droplets with the same attributes and position) and show that the result of Monte Carlo scheme agrees with the solution of the kinetic collection equation for the one component case. Nevertheless, for the Super Droplet method to reproduce accurately the solution of the kinetic collection equation, the number of species should be extremely large (around  $2^{17}$ ). As a consequence, the method doesn't reproduce well, for example, the time evolution of a monodisperse initial condition and will be discarded as an option to model the collection process for large coalescence volumes. In the grouping method (Ormel and Spaans, 2008) the species are divided into groups composed of identical particles. Thus, for the number of species:

$$N_i = w_i 2^{z_i} \quad (16)$$

Where  $w_i$  is number of groups, and  $z_i$  is the zoom number. Then, instead of tracking  $N_i$  droplets, we will simulate the collision between  $w_i$  groups, each containing  $2^{z_i}$  droplets. The number of groups will now determine the collision rate. The coagulation is accelerated significantly, because collisions are now between groups of particles, and not between individual particles. The total number of physical particles is:

$$N_T = \sum_{i=1}^{N_s} w_i 2^{z_i} \quad (17)$$

where  $N_s$  is the total number of species. The collision rates between groups of different species are calculated in the form (if  $z_i \leq z_j$ ):

$$a^G(i,j) = V^{-1} K(i,j) N_i N_j dt / 2^{z_i} \equiv \text{Pr}\{ \text{Probability that two groups of species } i \text{ and } j \text{ (for } i \neq j) \text{ with populations (number of particles) } N_i \text{ and } N_j \text{ will collide within the imminent time interval} \} \quad (18)$$

And the collision between groups of the same species:

$$a^G(i,i) = \frac{V^{-1} K(i,i) N_i (N_i - 1)}{2} / 2^{z_i - 1} \equiv \text{Pr}\{ \text{Probability that two groups of the same species } i \text{ with population (number of particles) } N_i \text{ collide within the imminent time interval} \} \quad (19)$$

In the general case  $z_i \leq z_j$ , then each  $i$  particle collides with  $2^{z_j - z_i}$   $j$  particles. After the collision event, only one group consisting of  $2^{z_i}$  particles is obtained. For the new particles, the mass of the  $k$ -component is calculated as:

$$m_{ki} + 2^{z_j - z_i} m_{kj} \quad (20)$$

The grouping algorithm in the form implemented in Ormel and Spaans (2008) is not feasible for incorporating into a microphysical framework, because the simulation results are the averages over several realizations, and we need a single realization and a constant time step for linking to a microphysical model. Thus, the modification of the Monte Carlo algorithm proposed by Sun et al. (2007) is also implemented for the grouping method. The algorithm can be summarized as follows:

1. At  $t=0$ , the event counter is set to zero and the initial number of species  $N_1, N_2, \dots, N_N$  are defined.
2. Set the zoom numbers for each species ( $N_i = w_i 2^{z_i}$ )
3. Determine the total number of group collisions ( $C_T^G$ ) in the time interval  $\Delta t$  by using the expression (where  $a^G(i,j)$  is calculated according to Eqs. 18 and 19) :

$$C_T^G = \frac{\Delta t \sum_{i=1}^{N_s} \sum_{j=1}^{N_s} a^G(i,j)}{V} \tag{21}$$

4. Generate  $C_T^G$  random ( $r_i$ ) numbers from a uniform distribution and determine the collision indexes from the relation:

$$\sum_{v=1}^{\mu-1} a_v^G < r_1 \alpha^G < \sum_{v=1}^{\mu} a_v^G \tag{22}$$

In (22),  $\alpha_v^G = a^G(i,j)$  and  $\alpha^G = \sum_{v=1}^{\frac{N(N+1)}{2}} a_v^G$ , where the index  $\{v\}$  defined the total collision space.

5. Reduce the number of groups for the colliding species:  $w_i = w_i - 1$ ,  $w_j = w_j - 1$ , and the number of physical particles for the species: If  $z_i \leq z_j$  then  $N_i = N_i - 2^{z_i}$  and  $N_j = N_j - 2^{z_i}$ . For the new species created in the collision the number of particles is increased by  $2^{z_i - z_i}$ .
6. Return to step 2.

The performance of the algorithm was checked again by comparison with the analytical solution for the sum kernel (Eqs.15 a, b). We have calculated the evolution of an initial monodisperse distribution of  $10^8$  droplets of  $14 \mu\text{m}$  in radius (droplet mass  $1.1494 \times 10^{-8}\text{g}$ ) in a cloud volume of  $10^6 \text{ cm}^3$ . As was pointed out, only a single stochastic experiment was run with a zooming factor ( $z_i$ ) of 10. Thus, the number of particles in each group was  $2^{10} = 1024$ . Figure 4 displays the comparison between the analytical and the MC total concentrations, indicating a very good correspondence between the two methods.

An additional simulation was performed, using the constant kernel, and the results compared with the analytical solution of the two-component kinetic collection equation:

$$\frac{\partial N(m,n;t)}{\partial t} = \frac{1}{2} \sum_{m'=0}^m \sum_{n'=0}^n K(m-m',n-n';m',n';t) N(m-m',n-n';t) N(m',n';t) - N(m,n;t) \sum_{m'=0}^{\infty} \sum_{n'=0}^{\infty} K(m,n;m',n') N(m',n';t) \tag{23}$$

In (23),  $N(m,n,t)$  is the average number of particles consisting of  $m$  and  $n$  monomers of the first and second kind respectively (with water mass from size bin  $m$  and aerosol mass from size bin  $n$ ). The water mass in size bin  $m$  equals the volume of a droplet in the smallest (monomer droplet) bin multiplied by  $m$ , the aerosol mass in size bin  $n$  equals the volume of an aerosol in the smallest bin (monomer aerosol) multiplied by  $n$ .

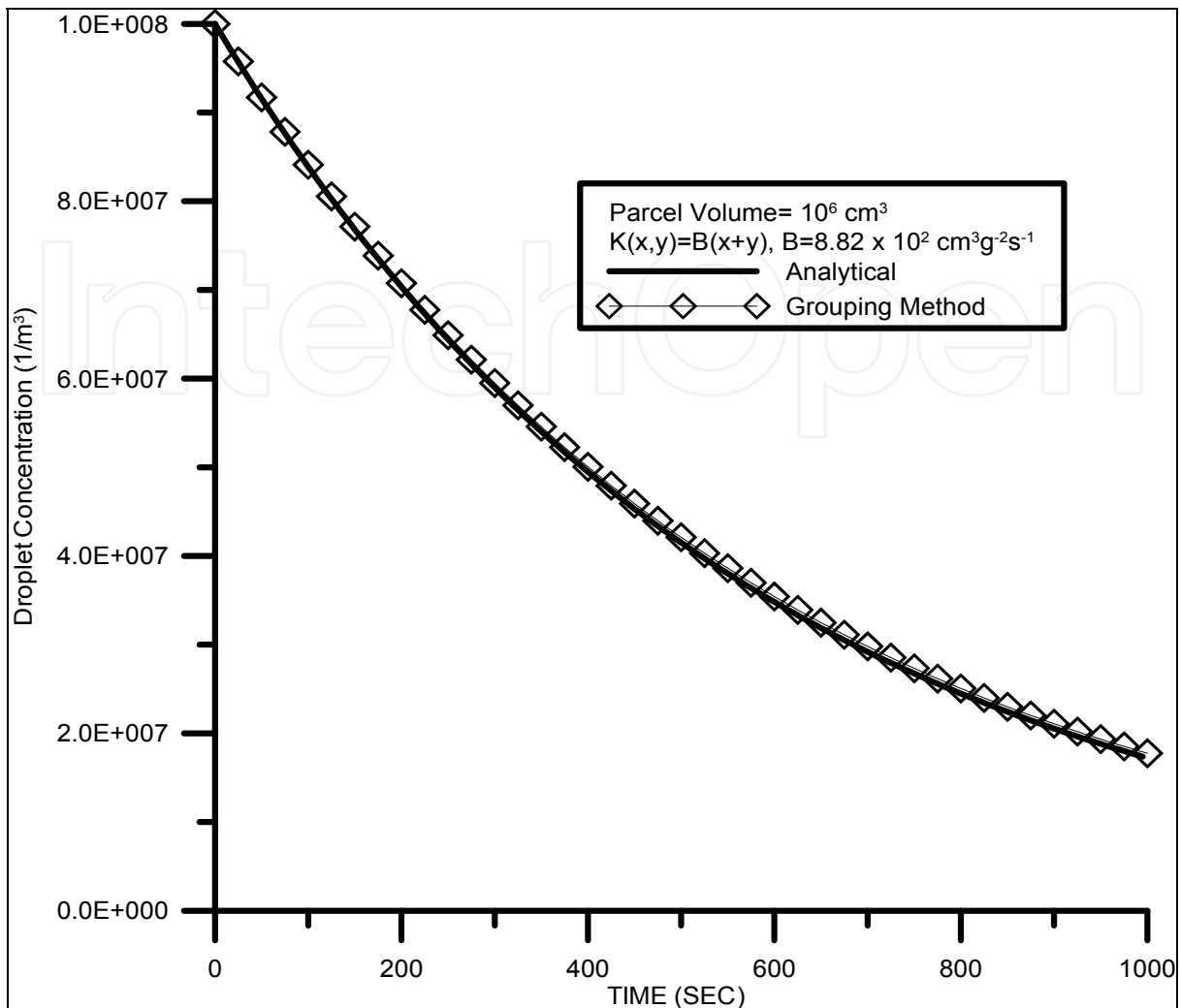


Fig. 4. Time evolution of the total number of particles obtained from the grouping method (diamonds), versus the analytical solution from the kinetic collection equation (solid line).

Solutions to (23) can be obtained for an important class of collection kernels, such as when the kernel depends only on the total number of monomers (droplets and aerosols) in each colliding particle. In this case:

$$K(m,n;m_1,n_1)=K(m+n,m_1+n_1) \quad (24)$$

Lushnikov (1975) constructed an explicit form for the composition distribution for this type of kernel, which corresponds to coagulation of initially monomeric particles. In this case  $N(1,0;0)=c_1$  and  $N(0,1;0)=c_2$ , corresponding to the situation with initially  $c_1$  droplets and  $c_2$  aerosols. The composition distribution may be expressed as (Lushnikov, 1975):

$$N(m,n;t)=\binom{m+n}{n}\left(\frac{c_1}{c_0}\right)^m\left(\frac{c_2}{c_0}\right)^n N(m+n,t) \quad c_0=c_1+c_2 \quad (25)$$

where  $\binom{m+n}{n}$  are the binomial coefficients, and  $N(m+n,t)$  is the number of particles composed of  $(m+n)$  monomers ( $m$  monomer droplets and  $n$  monomer aerosols). Lushnikov

(1975) showed that  $N(m+n,t)$ , for the type of kernels (24) is a solution of the one-component kinetic collection equation (1). For the constant kernel  $K(m,n;m_1,n_1)=A$  and a monodisperse initial distribution with concentration  $c_0$ , the analytical size distribution for the one-component KCE is:

$$N(i,t)=4c_0 \frac{(T)^{i-1}}{(T+2)^{i+1}} \quad \text{with} \quad T=Ac_0t \quad (26)$$

Then, for the constant kernel, the analytical solution of Eq. (23), calculated according to the expression (25) for the constant kernel  $K(m,n;m',n')=1.2 \times 10^{-4} (\text{cm}^3 \text{sec}^{-1})$  was compared with results of the Monte Carlo two-component simulation which was conducted for initially monomeric particles (droplets and aerosols) with concentrations  $c_1=30000$  and  $c_2=30000$  ( $N(1,0;0)=30 \times 10^3$  and  $N(0,1;0)=30 \times 10^3$ ). The initial volume was set equal to  $1000 \text{ cm}^3$ . The results are displayed in Figs. 5a,b. Again, a good agreement between the two approaches is found. These results support the validity of the grouping method for two-component stochastic coalescence.

#### 4. The multicomponent microphysical framework

The stochastic algorithm described in section 3 was incorporated into a multicomponent cloud microphysical framework. This particle-based cloud microphysical model will explicitly resolve the composition of individual droplets containing different types of CCN and is designed to accurately track the evolution by activation, condensation and coalescence of the composition of individual droplets with internally or externally mixed aerosols.

##### 4.1 Modeling of dynamical processes

The microphysical model is coupled with a simple parcel model. The air parcel is assumed to be adiabatic and homogeneous with no heat and mass exchange with the environment, with a pressure that adjusts instantaneously to that of the surrounding air, which is in hydrostatic equilibrium. The vertical velocity is prescribed. The set of equations for this case has the form (Pruppacher and Klett, 1997):

$$\frac{dT}{dt} = -\frac{gU}{c_{pa}} + \frac{L_e}{c_{pa}} C_{ph} \quad (27a)$$

$$C_w = \frac{dQ_L}{dt} \quad (27b)$$

$$\frac{dQ_V}{dt} = -C_w \quad (27c)$$

Where  $T$  is the temperature;  $U$ , the vertical velocity;  $g$ , the acceleration of gravity,  $c_{pa}$  the specific heat of air;  $L_e$ , the latent heat of evaporation;  $Q_V$  and  $Q_L$  are the water vapor and water mixing ratios and  $C_w$  is the rate of condensation. There is no sedimentation of drops with this simplified treatment of the dynamics.

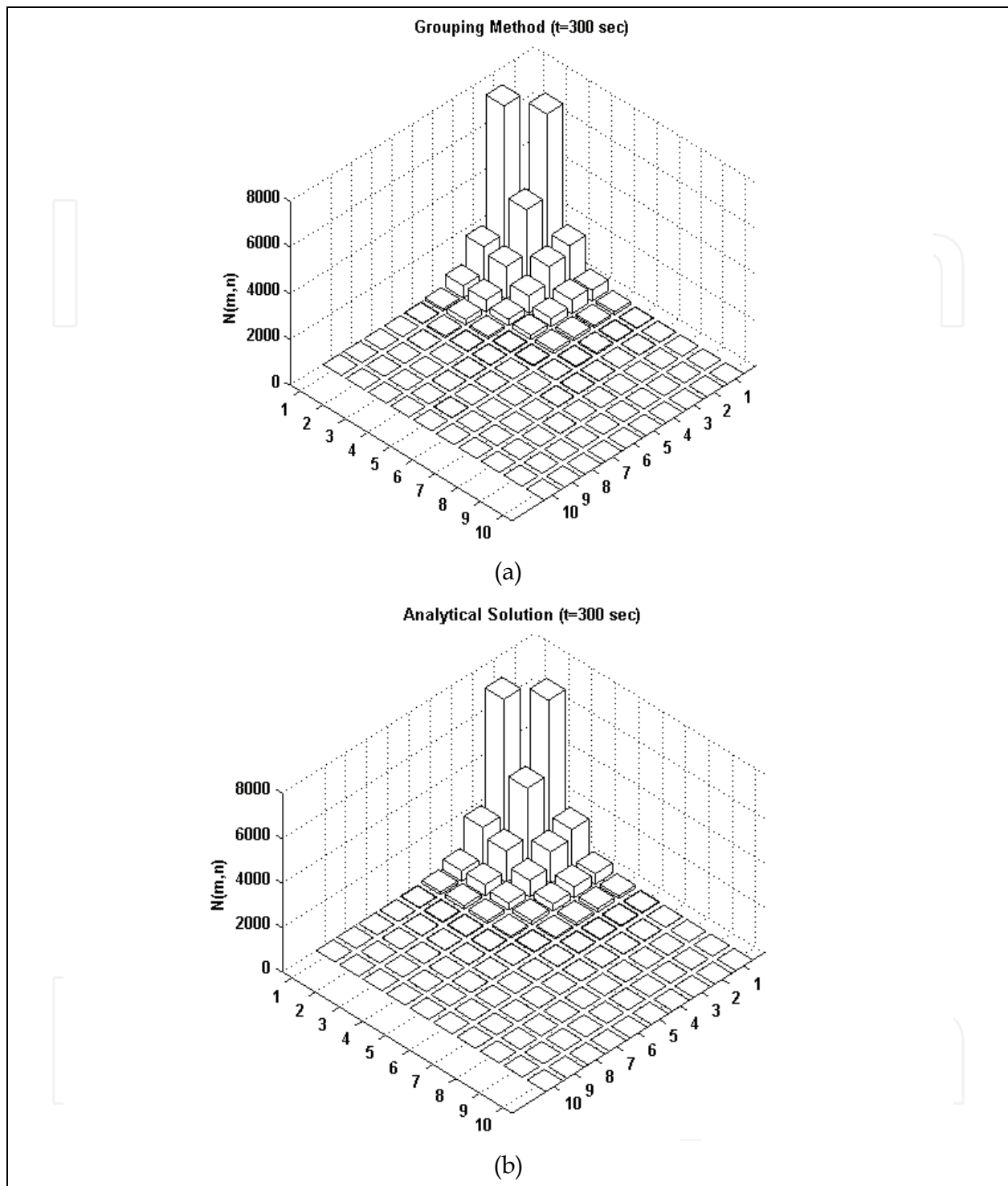


Fig. 5. Two dimensional droplet distribution  $N(m,n)$  for the constant kernel obtained by a) the grouping method and b) from the analytical solution of the two-component KCE. Simulations were conducted with initial conditions  $N(1,0)=30000$  and  $N(0,1)=30000$ .

#### 4.2 Condensation and evaporation of droplets

The usual form of the growth equation is not feasible for multicomponent microphysics. Therefore, we will consider the mass change of the species through the condensation -

evaporation process according to the modified form of the Köhler theory proposed by Mircea et al. (2002):

$$S = \frac{2\sigma M_w}{R_v T \rho_w r} - \frac{3\Phi_s M_w}{4\pi \rho_w r^3} \times \left( \sum_{i_{inorg}} \frac{v_i m_i}{M_i} + \sum_{j_{org}} \frac{v_j m_j}{M_j} \right) \tag{28}$$

This form of the Köhler equation takes into account the presence of multiple components (water soluble organic compounds,WSOC and inorganic salts) in the CCN. In (28)  $S$  is the supersaturation ratio,  $M_w$  and  $\rho_w$  are the molecular mass and density of water,  $\sigma$  is the surface tension,  $\Phi_s$  is the osmotic coefficient ( $\Phi_s=1$ ),  $R_v$  is the gas constant,  $T$  is the temperature, and  $r$  is the droplet radius. The number of dissociated ions, soluble mass and molecular mass respectively of the inorganic and organic components of CCN particles are represented by  $v_i, m_i, M_i$  and  $v_j, m_j, M_j$ . An ideal solution is assumed ( $\rho_s=\rho_w$ ).

Then, according to (28) the governing equation for diffusional growth of a water droplet of radius  $r$  is (Rogers and Yau, 1989):

$$r \frac{dr}{dt} = \frac{(S-1) - \frac{2\sigma M_w}{R_v T \rho_w r} + \frac{3\Phi_s M_w}{4\pi \rho_w r^3} \times \left( \sum_{i_{inorg}} \frac{v_i m_i}{M_i} + \sum_{j_{org}} \frac{v_j m_j}{M_j} \right)}{F_k + F_d} \tag{29}$$

$$F_k = \left( \frac{L}{R_v T} - 1 \right) \frac{L \rho_w}{kT} \tag{30}$$

$$F_d = \frac{\rho_w R_v T}{D e_s(T)} \tag{31}$$

Here  $S$  is the ambient, saturation ratio,  $F_k$  is represents the thermodynamic term associated with heat conduction,  $F_d$  is the term associated with vapor diffusion. In (30) and (31)  $R_v$  is the individual gas constant for water vapor,  $k$  is the coefficient of thermal conductivity of air,  $D$  is the molecular diffusion coefficient,  $L$  is the latent heat of vaporization and  $e_s(T)$  is the saturation vapor pressure.

In order to allow larger integration steps for the condensation process an implicit Euler discretization scheme was adopted:

$$\frac{r_{n+1}^2 - r_n^2}{2\Delta t} = \frac{(S-1) - \frac{a}{r_{n+1}} + \frac{b}{r_{n+1}^3}}{F_k + F_d} \tag{32}$$

Where  $a = \frac{2\sigma M_w}{R_v T \rho_w}$  and  $b = \frac{3\Phi_s M_w}{4\pi \rho_w} \times \left( \sum_{i_{inorg}} \frac{v_i m_i}{M_i} + \sum_{j_{org}} \frac{v_j m_j}{M_j} \right)$

The droplet radius  $r_{n+1}$  in the  $n+1$  iteration were calculated with the Newton Raphson method. In the model there is no need to parameterize the activation process since the equation (29) was applied to both the unactivated equilibrium droplets and activated drops. In the first case, the numerical solution of (29) gives the equilibrium radius for a given saturation ratio, which satisfies the Köhler equation:



$$S=1+\frac{a}{r_{n+1}}-\frac{b}{r_{n+1}^3} \quad (33)$$

### 4.3 Treatment of supersaturation

For calculating the saturation ratio, a time splitting procedure was used, and the evolution of the variables due to dynamical processes is calculated first:

$$T^*=T^n-\Delta t \times \frac{gU}{c_{pa}}, \quad Q_V^*=Q_V^n \quad (34)$$

There is no change in the water vapor mixing ratio due to dynamics because the air parcel is assumed to be adiabatic with no mass exchange with the environment. By taking into account the microphysical processes, the temperature and water vapor at the  $n+1$  time step are calculated as:

$$T^{n+1}=T^*+\frac{\Delta t}{c_{pe}} \times L_e \frac{d\chi}{dt}, \quad Q_V^{n+1}=Q_V^*-\Delta t \times \frac{d\chi}{dt} \quad (35)$$

Where  $\Delta t$  is the time step, and  $d\chi/dt$  is the condensation rate, which is calculated from the expression:

$$\frac{d\chi}{dt}=\frac{\rho_w}{\rho_a} \sum_i N_i 4\pi r_i^2 \frac{dr_i}{dt} \quad (36)$$

Here,  $N_i$  is the total number of droplets (unactivated and activated) for the species with index  $i$ ,  $r_i$  is the droplet radius,  $\rho_w$  and  $\rho_a$  are the water and air densities, and  $dr_i/dt$  is calculated from (29). The saturation ratio at the  $n+1$  time step can be found from the equation (Hall, 1980):

$$S^{n+1}=\frac{Q_V^{n+1}}{Q_{VS}^{n+1}(p, T^{n+1})}=\frac{Q_V^*-\Delta t \times \frac{d\chi}{dt}}{T^*+\frac{\Delta t}{c_p} \times L_e \frac{d\chi}{dt}} \quad (37)$$

Which is solved iteratively using the secant method. In (37) the condensation rate  $d\chi/dt$  is evaluated at  $\bar{S}_m=0.5(S^n+S_m^{n+1})$  and  $S_m^{n+1}$  is iteratively determined until  $|S_m^{n+1}-S_m^n|<10^{-8}$ . After that, the saturation ratio  $\bar{S}_m=0.5(S^n+S_m^{n+1})$  is applied directly to the growth equations that are integrated implicitly.

## 5. Simulation results

The parcel model described in section 4 was used to simulate the microphysical evolution of an orographic cloud sampled on November 20, 2007, located in the northwest corner of Nebraska.

The initial CCN distribution for the simulation represented an external mixture of 3 different composition categories: pure sodium chloride: (NaCl), oxalic acid-elemental carbon

mixture (OC-EC) and ammonium sulfate-elemental carbon:  $(\text{NH}_4)_2\text{SO}_4$ -EC (Figure 6). The initial CCN total number concentration was  $531 \text{ cm}^{-3}$ . The (OC-EC) and  $(\text{NH}_4)_2\text{SO}_4$ -EC particles were assumed to consist of 90% water soluble materials, with a 10% of elemental carbon. NaCl particles were assumed 100% solubility. The smallest NaCl aerosol particles require a supersaturation of 0.33 % to activate, a value that was never exceeded in the simulations (see Figure 7b). The largest critical supersaturation for the OC-EC particles is 0.24 %.

The air parcel ascends with a constant vertical velocity of  $0.5 \text{ ms}^{-1}$  from cloud base at  $-8^\circ\text{C}$  and 764 hPa. The calculation starts at 98% relative humidity with moist adiabatic lapse rate. A cloud height from the cloud base of 200 m was simulated. The parcel volume was assumed to be  $10^5 \text{ cm}^3$  (100 liters), with zoom numbers for the grouping algorithm  $z_i=5$  for all the species (which means we have  $2^5=32$  droplets in each group), and a time step of  $\Delta t=1$  sec. Therefore, the initial number of particles in the simulation was  $531 \times 10^5$ .

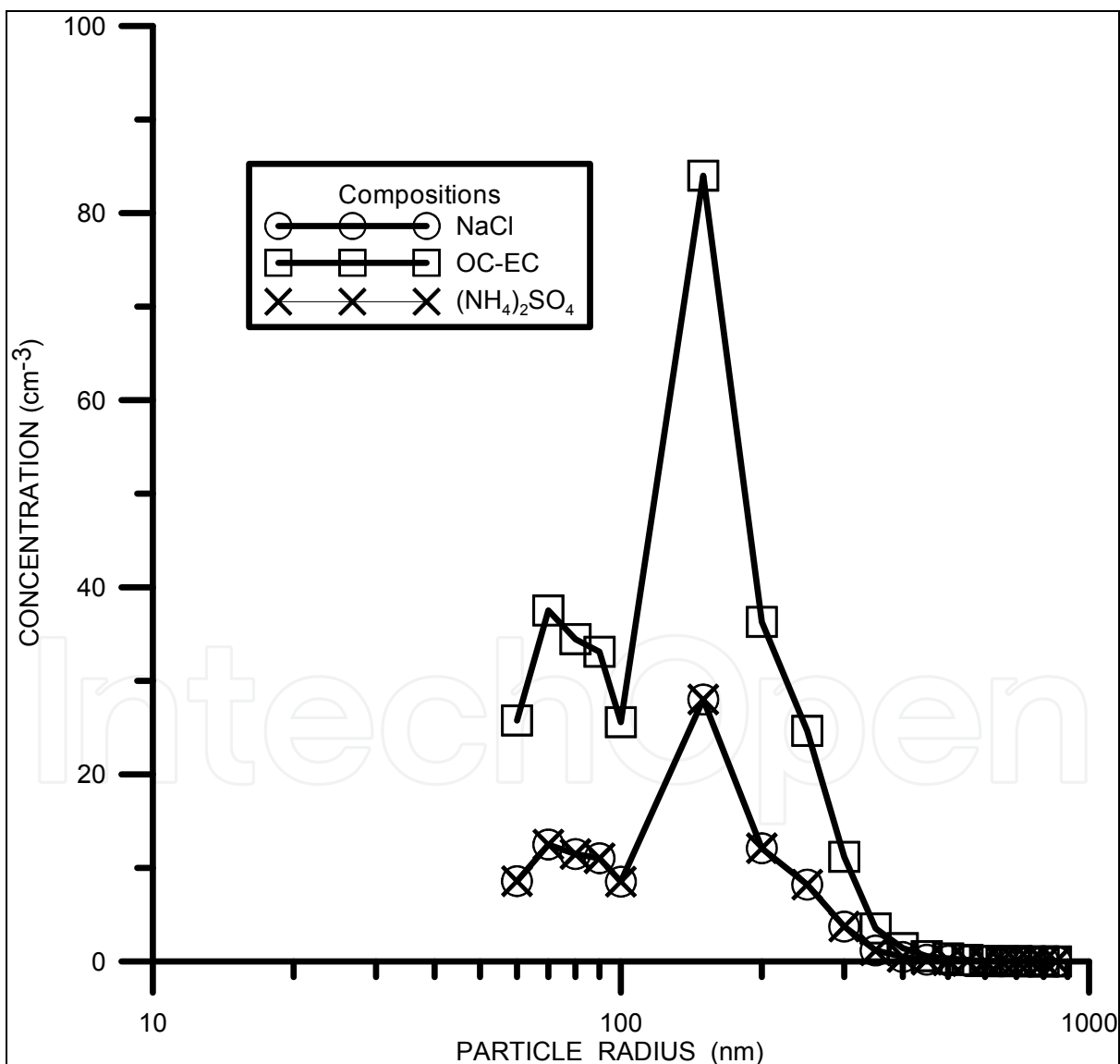


Fig. 6. CCN size distributions that served as basis of calculations for the three different compositions.

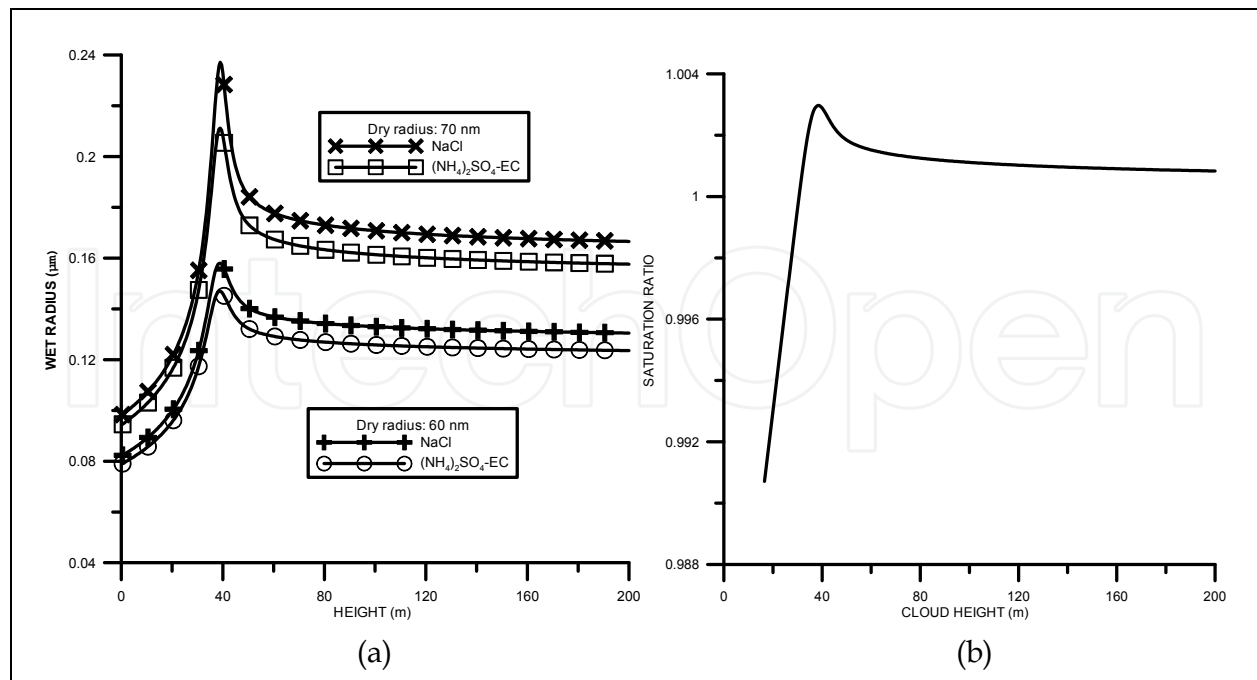


Fig. 7. Wet radius for interstitial aerosols as a function of height above cloud base, and supersaturation profile for the simulated cloud.

In a first experiment, the size distribution was allowed to evolve only by nucleation and condensation. The vertical profile of supersaturation obtained in this simulation is shown in Figure 7b. As can be observed, the maximum supersaturation is about 0.3%.

After peak supersaturation is reached, the aerosol number total concentration decreased from  $531 \text{ cm}^{-3}$  to  $42 \text{ cm}^{-3}$  due to nucleation scavenging (a 92% decrease), in agreement with field observations of Hegg & Hobbs (1983). The number concentration of the different components show the following evolution: the NaCl and  $(\text{NH}_4)_2\text{SO}_4\text{-EC}$  aerosol particles decreased by 80% (from 106 to  $21 \text{ cm}^{-3}$ ) and 100% of the OC-EC aerosol particles were nucleated. This is consistent with the cloud supersaturation spectra (CSS) which have maximum critical supersaturations of 0.25% for the aerosol particles with OC-EC compositions. Consequently, all the particles in this category get activated after the maximum supersaturation of 0.3% is reached. The aerosol particles that were not activated to droplets remain as interstitial aerosols and in equilibrium with ambient supersaturation conditions (Figure 6a).

Figure 8 shows the evolution as a function of height above cloud base for the largest droplet in each of the three aerosol composition species. The droplets formed on the (OC-EC) CCN achieve a larger size than the droplets that contain the inorganic salts.

In a second simulation, the size distribution was allowed to evolve by activation, condensation and the collision-coalescence process in the manner described in section 4. The zoom numbers were assumed to be  $z_i=5$  for all the species (which means we have  $2^5=32$  droplets in each group), with a time step of  $\Delta t=1$  sec. Despite the large number of particles for the parcel under analysis, the coalescence was almost negligible with a maximum of 3 collision events per time step. Nevertheless, at the end of the parcel ascent the number of species was incremented up to 593. The huge increment in the number of species (from 57 to 593) is only explained by the coalescence, since the condensation and activation processes

conserved the number of species. Due to the fact that we have a four-component system (droplet radius and three types of aerosols inside droplets), practically every collision leads to the formation of a new species. The maximum droplet radius was  $7.35 \mu\text{m}$  with an aerosol with composition OC-EC and radius  $0.3999 \mu\text{m}$ . An additional simulation was performed with a parcel volume of  $5000 \text{ cm}^3$  and a zoom factor of  $z=0$  for all the species in order to compare with the previous simulation. In that case we were considering collisions between particles, not between groups. The same maximum droplet radius was obtained as a result of the simulation. These preliminary findings are encouraging and show the potential of this modeling approach.

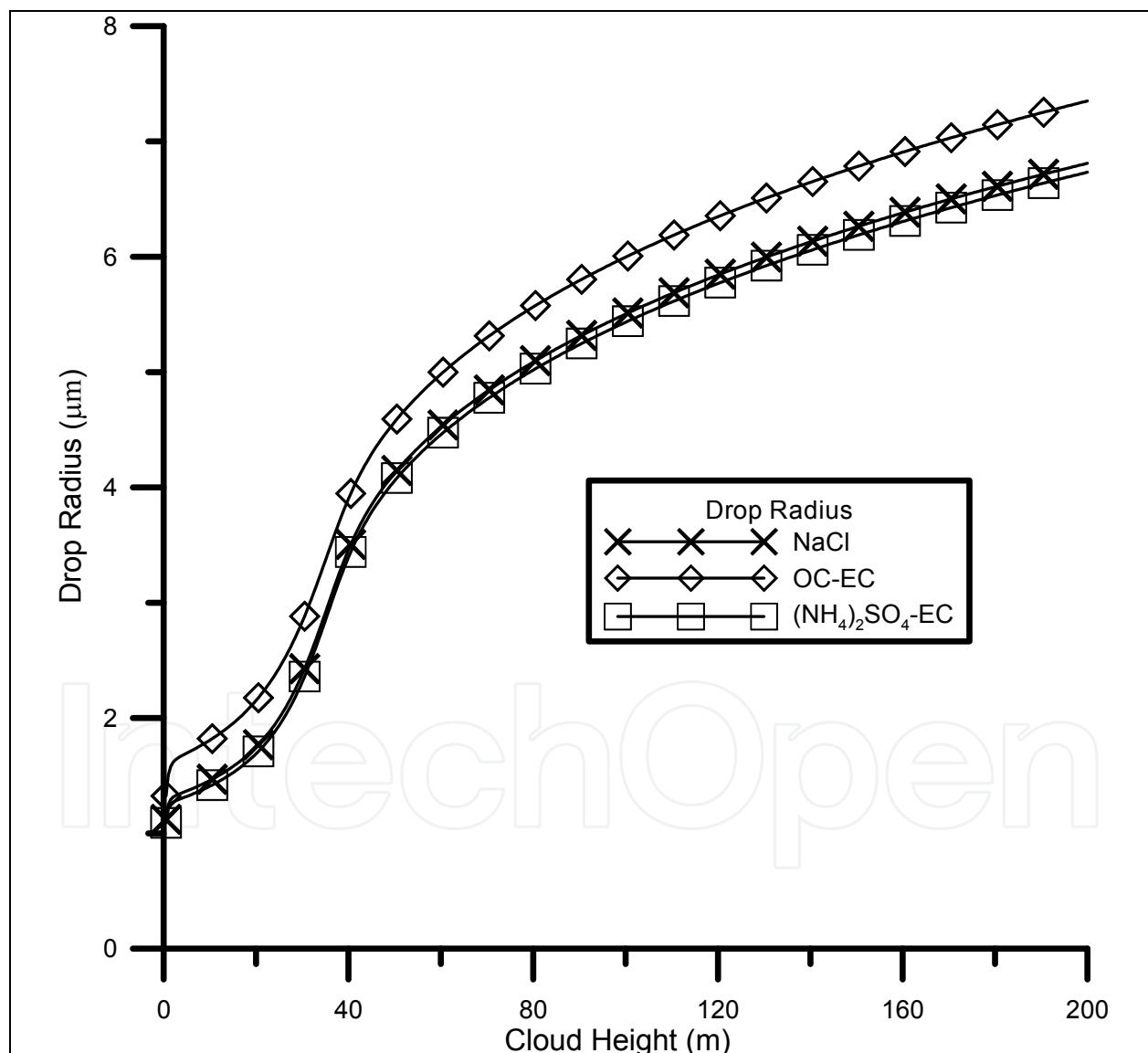


Fig. 8. Largest droplet radius for the activated species.

## 6. Conclusions

In this work, a novel Monte Carlo multicomponent framework for the collection process was introduced, and its characteristics discussed in detailed. The Monte Carlo algorithm is based on the grouping method proposed by Ormel and Spaans (2008), and allows accurate simulation of the coalescence process in large cloud volumes with reasonable cost in computation. Therefore, it can be a useful tool to simulate microphysical evolution in cloud models with complex dynamics.

The applicability of the Monte Carlo grouping method was demonstrated by linking the stochastic framework with a microphysical model with simple dynamics, and presenting very preliminary results of an orographic cloud formation with four component microphysics.

Simulation results suggest that the Monte Carlo grouping method can be computationally more efficient than the deterministic framework (based on the solution of the KCE), when the number of components of the system is larger than 2. Then, it is expected to be more feasible for modeling complicated microphysics, and provides us with a new tool to solve open problems in cloud modeling.

Even though a more thorough validation of the method is still needed, we believe that this stochastic algorithm will prove to be a useful new approach to simulations of multicomponent microphysics. It is particularly applicable to studies of cloud and aerosol interactions with multiple types of CCN, the modeling of collection process in mixed phase clouds and cloud chemistry.

As a future work, an important effort will be required to extend this method to model the microphysical evolution of mixed phase clouds, and to include the chemical processes. This work attempts to be a first step toward the accomplishment of these goals.

## 7. Acknowledgements

The authors are grateful to LUFAC Computación SA de CV for funding the publication of this work.

## 8. References

- Alfonso, L. & Raga, G.B. (2004). The influence of organic compounds in the development of precipitation acidity in maritime clouds. *Atmos. Chem. Phys.*, 4, 1097-1111.
- Alfonso, L.; Raga G.B., & Baumgardner, D. (2008). The validity of the kinetic collection equation revisited.-Part II.: Simulations for the hydrodynamic kernel. *Atmos. Chem. Phys.*, 8, 969-982.
- Alfonso, L.; Raga, G.B. & Baumgardner, D. (2009). Monte Carlo simulations of two component droplet growth by stochastic coalescence. *Atmos. Chem. Phys.*, 9, 2141-1251.
- Alfonso, L.; Raga G.B., & Baumgardner, D. (2010). The validity of the kinetic collection equation revisited.-Part II.: Simulations for the hydrodynamic kernel. *Atmos. Chem. Phys.*, 10, 6219-6240.
- Bayewitz, M.H.;Ye Yerushalmi; J., Katz, S. & Shinnar, R. (1974). The extent of correlations in a stochastic coalescence process, *J. Atmos. Sci.*, 31, 1604-1614.

- Berry E.X. & Reinhardt R.L. (1974). An analysis of cloud drop growth by collection. Part I. Double distributions. *J. Atmos. Sci.*, 1974, 31, 1814-1824.
- Bott, A.A. (2000). A flux method for the numerical solution of the stochastic collection equation: Extension to two-dimensional particle distribution. *J. Atmos. Sci.*, 57, 284-294.
- Bott, A.A. (1998). A flux method for the numerical solution of the stochastic collection equation. *J. Atmos. Sci.*, 55, 2284-2293.
- Drake, R.L. (1972). The scalar transport equation of coalescence theory: Moments and kernels, *J. Atmos. Sci.*, 29, 537-547.
- Flossmann, A. I. (1994). A 2-D spectral model simulation of the scavenging of gaseous and particulate sulfate by a warm marine cloud. *Atmos. Res.*, 32, 233-248.
- Feingold, G. & Kreidenweiss, S.M. (2002). Cloud processing of aerosol as modeled by a large eddy simulation with coupled microphysics and chemistry. *J. Geophys. Res.*, 107, 4687.
- Gillespie, D. T. (1976). A general method for numerically simulating the stochastic time evolution of coupled chemical reactions. *J. Comput. Phys.*, 22, 403-434.
- Hegg, D.A. & Hobbs, P.V. (1983). Preliminary measurements on the scavenging of sulfate and nitrate by clouds. *Precipitation scavenging, dry deposition and resuspension. Vol. I.*, Elsevier Science, 78-89.
- Inaba, S. ; Tanaka, H.; Ohtsuki, K. & Nakazawa, K. (1999). High-accuracy statistical simulation of planetary accretion: I. Test of the accuracy by comparison with the solution to the stochastic coagulation equation, *Earth Planet Space*, 51, 205-217.
- Jacobson, M.Z. (1999). *Fundamentals of atmospheric modeling*. Cambridge University Press, 656 pp., ISBN 0521-63717.
- Khain, A.P. & Sednev, I., (1995). Simulation of hydrometeor size spectra evolution by water-water, ice-water and ice-ice interactions. *Atmos. Res.*, 36, 107-138.
- Long, A.B. (1974). Solutions to the droplet collection equation for polynomial collection kernels, *J. Atmos. Sci.*, 31, 1040-1051.
- Lushnikov, A.A. (1975). Evolution of coagulating systems III: Coagulating mixtures, *J. Coll. Int. Sci.*, 54, 94-101.
- Mircea, M.; Facchini, M.M.; Decesari, S.; Fuzzi, S. & Charlson, R.J. (2002). The influence of organic aerosol component on CCN supersaturation spectra for different aerosol types. *Tellus*. 54B, 74-81.
- Ormel, C.W. & Spaans, M. (2008). Monte Carlo simulation of particle interactions at high dynamic range: Advancing beyond the Googol. *ApJ.*, 684, 1291.
- Pruppacher, H.R. & Klett, J.D. (1997). *Microphysics of clouds and precipitation*, Kluwer Academic Publishers, ISBN 0-7923-4211-9.
- Rogers, R.R. & Yau, M.K. (1989). *A short course in cloud physics*, Elsevier, New, York.
- Shima, S.I.; Kusano, K.; Kawano, A.; Sugiyama, T. & Kawahara, S. (2005). Super-Droplet method for the numerical simulation of Clouds and Precipitation: A particle-based microphysics model coupled with non-hydrostatic model. *Arxiv:physics/0701103v1*.

- Sun, Z.; Axelbaum, R. & Huertas, J. (2007). Monte Carlo simulation of multicomponent aerosols undergoing simultaneous coagulation and condensation, *J. Aer. Sci. Tech.*, 38, 963-971.
- Scott, W.T. (1968). Analytic studies of cloud droplet coalescence, *J. Atmos. Sci.*, 25, 54-65.
- Tanaka, H. & Nakazawa, K. (1994). Validity of the statistical coagulation equation and runaway growth of protoplanets, *Icarus*, 107, 404-412.
- Wang, L.P.; Xue, Y.; Ayala, O. & Grabowski, W.W. (2006). Effect of stochastic coalescence and air turbulence on the size distribution of cloud droplets, *Atmos. Res.*, 82, 416-432.

IntechOpen



## **Applications of Monte Carlo Method in Science and Engineering**

Edited by Prof. Shaul Mordechai

ISBN 978-953-307-691-1

Hard cover, 950 pages

**Publisher** InTech

**Published online** 28, February, 2011

**Published in print edition** February, 2011

In this book, Applications of Monte Carlo Method in Science and Engineering, we further expose the broad range of applications of Monte Carlo simulation in the fields of Quantum Physics, Statistical Physics, Reliability, Medical Physics, Polycrystalline Materials, Ising Model, Chemistry, Agriculture, Food Processing, X-ray Imaging, Electron Dynamics in Doped Semiconductors, Metallurgy, Remote Sensing and much more diverse topics. The book chapters included in this volume clearly reflect the current scientific importance of Monte Carlo techniques in various fields of research.

### **How to reference**

In order to correctly reference this scholarly work, feel free to copy and paste the following:

Lester Alfonso, Graciela Raga and Darrel Baumgardner (2011). A Monte Carlo Framework to Simulate Multicomponent Droplet Growth by Stochastic Coalescence, Applications of Monte Carlo Method in Science and Engineering, Prof. Shaul Mordechai (Ed.), ISBN: 978-953-307-691-1, InTech, Available from: <http://www.intechopen.com/books/applications-of-monte-carlo-method-in-science-and-engineering/a-monte-carlo-framework-to-simulate-multicomponent-droplet-growth-by-stochastic-coalescence>

# **INTECH**

open science | open minds

### **InTech Europe**

University Campus STeP Ri  
Slavka Krautzeka 83/A  
51000 Rijeka, Croatia  
Phone: +385 (51) 770 447  
Fax: +385 (51) 686 166  
[www.intechopen.com](http://www.intechopen.com)

### **InTech China**

Unit 405, Office Block, Hotel Equatorial Shanghai  
No.65, Yan An Road (West), Shanghai, 200040, China  
中国上海市延安西路65号上海国际贵都大饭店办公楼405单元  
Phone: +86-21-62489820  
Fax: +86-21-62489821



© 2011 The Author(s). Licensee IntechOpen. This chapter is distributed under the terms of the [Creative Commons Attribution-NonCommercial-ShareAlike-3.0 License](#), which permits use, distribution and reproduction for non-commercial purposes, provided the original is properly cited and derivative works building on this content are distributed under the same license.

IntechOpen

IntechOpen